Thrust belts of the southern Central Andes: Along-strike variations in shortening, topography, crustal geometry, and denudation

Laura Giambiagi[1,†], José Mescua[1], Florencia Bechis[2,†], Andrés Tassara[3,†], and Greg Hoke[4]

[1]*Centro Científico y Tecnológico CCT–Mendoza, Consejo Nacional de Ciencia y Tecnología (CONICET), Parque San Martín s/n, 5500 Mendoza, Argentina*

[2]*CONICET–IIDyPCA (Instituto de Investigaciones en Diversidad Cultural y Procesos de Cambio), Universidad Nacional de Río Negro, Sarmiento Inferior 3974, CP 8400, San Carlos de Bariloche, Argentina*

[3]*Departamento de Ciencias de la Tierra, Universidad de Concepción, Victor Lamas 1290, Concepción, Chile*

[4]*Department of Earth Sciences, Syracuse University, Syracuse, New York 13244, USA*

ABSTRACT

The Andean fold-and-thrust belts of west-central Argentina (33°S and 36°S), above the normal subduction segment, present important along-strike variations in mean topographic uplift, structural elevation, amount and rate of shortening, and crustal root geometry. To analyze the controlling factors of these latitudinal changes, we compare these parameters and the chronology of deformation along 11 balanced crustal cross sections across the thrust belts between 70°W and 69°W, where the majority of the upper-crustal deformation is concentrated, and reconstruct the Moho geometry along the transects. We propose two models of crustal deformation: a 33°40′S model, where the locus of upper-crustal shortening is aligned with respect to the maximum crustal thickness, and a 35°40′S model, where the upper-crustal shortening is uncoupled from the lower-crustal deformation and thickening. This degree of coupling between brittle upper crust and ductile lower crust deformation has strong influence on mean topographic elevation. In the northern sector of the study area, an initial thick and felsic crust favors the coupling model, while in the southern sector, a thin and mafic lower crust allows the uncoupling model.

Our results indicate that interplate dynamics may control the overall pattern of tectonic shortening; however, local variations in mean topographic elevation, deformation styles, and crustal root geometry are not fully explained and are more likely to be due to upper-plate lithospheric strength variations.

†E-mails: lgiambiagi@mendoza-conicet.gob.ar; florbechis@gmail.com; andrestassara@udec.cl.

INTRODUCTION

The Central Andes are a linear orogenic belt resulting from the subduction of the Nazca oceanic plate beneath the South American continental plate. Although they are considered to be the result of compression and uplift during three main deformational events that occurred from Cretaceous to Quaternary times (Mpodozis and Ramos, 1989), the majority of the crustal thickness and topographic uplift were achieved during the Miocene–Quaternary period. During this time, shortening in the orogen was mostly localized in the foreland thrust belts, which could account for at least two-thirds (Sheffels, 1990) to four-fifths of the total crustal shortening (Farías et al., 2010) in the Central and southern Central Andes, respectively.

Despite an apparent simplicity of the connection between subduction of an oceanic plate under the South American continent and tectonic shortening, the mechanisms that connect subduction to mountain building and surface uplift are widely debated. The key challenge is to understand the mechanisms responsible for crustal shortening and topographic uplift, and the relationship between these two phenomena.

Here, we study the southern segment of the Central Andes, where an abrupt change in horizontal shortening and mean topographic elevation occurs, while the width of the orogen and the maximum crustal thickness do not vary significantly (Fig. 1). The cause of the southward decrease in topography and tectonic shortening is debated, and numerous controls have been assigned to this phenomenon, such as variation in subduction dynamics and age and geometry of the slab (e.g., Jordan et al., 1983; Ramos et al., 2004; Ramos, 2010), rheological and inherited fabric of the South American plate (e.g., Ramos et al., 2004), and climate variations (e.g., Lamb and Davis, 2003). It is clear from all these studies that one factor alone cannot account for the latitudinal variations in deformation and topographic uplift in the Central Andes, but the degree of influence that these parameters have in Andean mountain building remains unclear. A crucial problem in understanding these mechanisms is distinguishing between the effects of subduction stress-building processes and those associated with upper-plate strength variations.

The aim of this paper is threefold: (1) analyze the distribution of horizontal shortening, crustal thickness and geometry, mean denudation, and mean topographic uplift; (2) explore the feedback mechanisms between these features; and (3) evaluate the potential controlling processes and their degree of influence. We approach this problem by identifying spatial and temporal patterns and magnitudes of deformation and crustal root geometry, combined with kinematic reconstructions. The study area lies immediately to the south of the flat-slab segment, and the Nazca plate is subducting at a similar rate and dip along the study area (Fig. 1). Therefore, the subduction kinematic patterns, such as convergence rate, obliquity, and topographic features, can be neglected. We argue that the amount of shortening has been shaped in large part by boundary conditions of the subduction system, but second-order features respond to the geological history of the upper plate, which determines its strength.

METHODOLOGY

We present five new balanced cross sections, 73 km long, and integrate them with six published ones (Giambiagi et al., 2003, 2009) using the academic license for MOVE software. We used available isotopic ages and provenance data to estimate onset and end of activity for

GSA Bulletin; July/August 2012; v. 124; no. 7/8; p. 1339–1351; doi:10.1130/B30609.1; 7 figures.

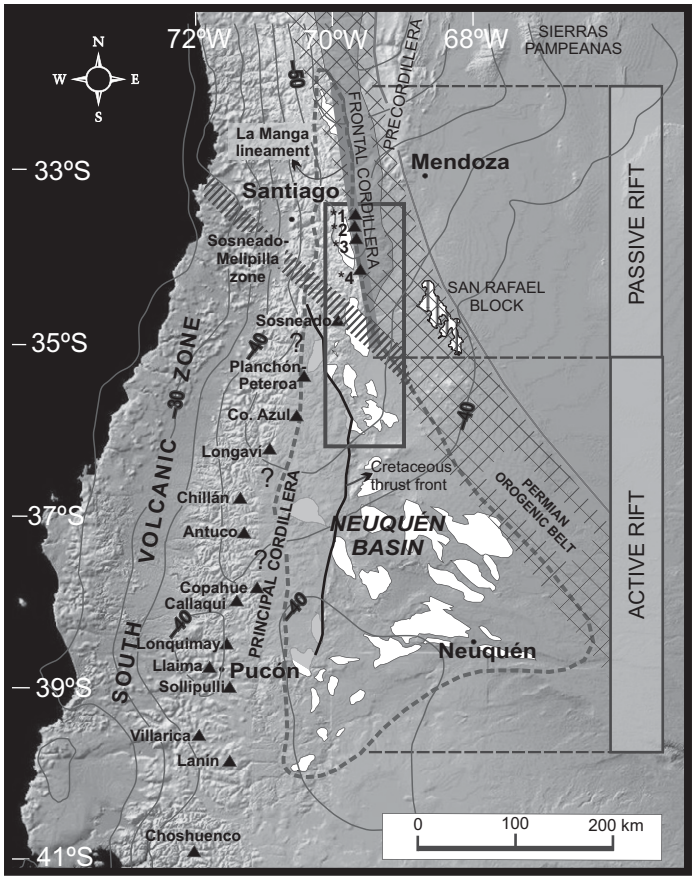

Figure 1. Shaded relief map of the Andes from 31°S to 41°S showing the study area (rectangle). The figure highlights the present-day Andean morphostructural units of the Principal Cordillera, Frontal Cordillera, Precordillera, Sierras Pampeanas, and San Rafael block, and pre-Andean morphostructural zones, such as the Mesozoic Neuquén Basin (dashed gray line); Late Cretaceous orogenic thrust front (solid gray line; modified from Mescua, 2010), and the Permian San Rafael orogeny located in a preexisting Paleozoic crustal anisotropy (squared area; modified from Giambiagi et al., 2011). Dark gray shows the Upper Triassic–Lower Jurassic depocenters of the Neuquén Basin. Contour lines indicate the Moho thickness taken from Tassara et al. (2006). Hachured zone trending NW and crossing the study area at the latitudes between 34°40′S and 35°20′S corresponds to a transitional zone between northern and southern sectors, where a variety of along-strike changes in Andean and pre-Andean features took place. Volcanoes: *1—Tupungato, *2—Marmolejo, *3—San José, and *4—Maipo.

each principal structure. Our values can be taken as a proxy for total crustal shortening, because the Chilean slope of the orogen has undergone little contraction in Neogene time. To explore latitudinal changes in present mean elevations along the thrust belts, we calculated along-strike topographic variations from the 3 arc-second Shuttle Radar Topography Mission (SRTM) digital elevation model (DEM). The data were processed to obtain 10-km-wide swaths for each structural cross section (Fig. 2), extending 5 km north and south of the latitude of the cross section. Pliocene–Quaternary volcanic edifices were masked to take into account only structurally built topography. To estimate denudation, a mean value was calculated for each cross section. For this, we used the reconstruction of the structures modeled in each cross section that reached higher than the present topography. This methodology provides minimum values, since some eroded thrust sheets could not be reconstructed.

Figure 2 (*on following page*). (A) Simplified geological map based on detailed compilations from Giambiagi et al. (2003, 2008, 2009), Silvestro et al. (2005), Yagupsky et al. (2008), Mescua and Ramos (2009), Mescua (2010), Bechis et al. (2010), and Turienzo (2010). This earlier information has been supplemented with new field mapping. (B) Balanced cross-sections A–K of the southern Central Andes between 33°30′S and 36°10′S. FTB—fold-and-thrust belt; FS—fault system.

In order to compare our estimates of geological shortening and denudation at the surface with the crustal-scale structure of the orogen, we consider the three-dimensional (3-D) density model of the Nazca plate and the Andean margin (Tassara and Echaurren, 2012). This model integrates most of the published geophysical information related to the internal structure of the subducted slab and the South American plate; a particularly relevant feature for us is the geometry of the Moho, which is well constrained in our study region from results of a number of seismic experiments (for a complete list of references, see Tassara et al., 2006).

TECTONIC AND GEOLOGICAL SETTING

The prolonged history of convergence against the Pacific edge of Gondwana resulted in several episodes of contractional, extensional, and strike-slip deformation, most of which were coeval with active subduction. Crustal heterogeneities that developed prior to the Andean orogeny have long been recognized as major features controlling subsequent deformation. Particularly in the Andean segment between 33°S and 36°S, Paleozoic contractional and Mesozoic extensional processes created anisotropies and weakness zones that later controlled lithospheric strength and structural styles during the Neogene compressive deformation.

Paleozoic Terrane Collision, Subduction, and Mountain Building

The early Paleozoic tectonic history of the southwestern margin of South America was mainly controlled by subduction process and the accretion of exotic terranes (e.g., Ramos, 1988). The late Paleozoic tectonic cycle began with the inception of subduction along the present continental margin. In Early Permian times, a widespread contractional event generated a wide NW- to NNW-trending orogenic belt (Azcuy and Caminos, 1987) and significant crustal

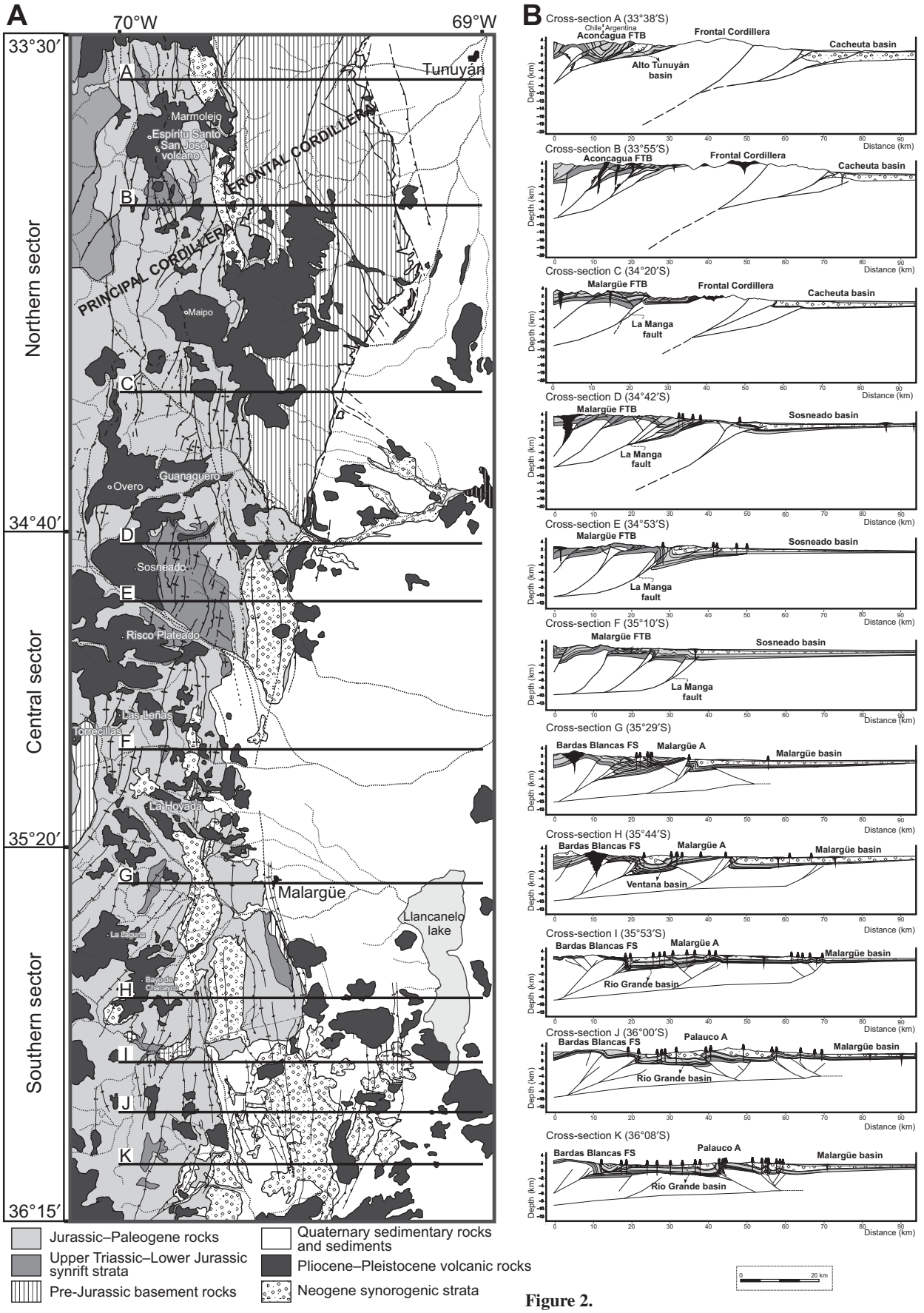
A
70°W
69°W
33°30′
34°40′
35°20′
36°15′
Northern sector
Central sector
Southern sector
Tunuyán
Marmolejo
Espíritu Santo
San José volcano
FRONTAL CORDILLERA
PRINCIPAL CORDILLERA
Maipo
Guanaguero
Overo
Sosneado
Risco Plateado
Las Leñas
Torrecillas
La Hoyada
Malargüe
Llancanelo lake
La Laguna
Barda de Chacaycó
A
B
C
D
E
F
G
H
I
J
K
Jurassic–Paleogene rocks
Upper Triassic–Lower Jurassic synrift strata
Pre-Jurassic basement rocks
Quaternary sedimentary rocks and sediments
Pliocene–Pleistocene volcanic rocks
Neogene synorogenic strata
B
Cross-section A (33°38′S)
Chile
Argentina
Aconcagua FTB
Frontal Cordillera
Cacheuta basin
Alto Tunuyán basin
Cross-section B (33°55′S)
Aconcagua FTB
Frontal Cordillera
Cacheuta basin
Cross-section C (34°20′S)
Malargüe FTB
Frontal Cordillera
Cacheuta basin
La Manga fault
Cross-section D (34°42′S)
Malargüe FTB
Sosneado basin
La Manga fault
Cross-section E (34°53′S)
Malargüe FTB
Sosneado basin
La Manga fault
Cross-section F (35°10′S)
Malargüe FTB
Sosneado basin
La Manga fault
Cross-section G (35°29′S)
Bardas Blancas FS
Malargüe A
Malargüe basin
Cross-section H (35°44′S)
Bardas Blancas FS
Malargüe A
Malargüe basin
Ventana basin
Cross-section I (35°53′S)
Bardas Blancas FS
Malargüe A
Malargüe basin
Río Grande basin
Cross-section J (36°00′S)
Palauco A
Bardas Blancas FS
Malargüe basin
Río Grande basin
Cross-section K (36°08′S)
Palauco A
Bardas Blancas FS
Malargüe basin
Río Grande basin
Depth (km)
Distance (km)
0
20 km

Figure 2.

thickening (Llambías and Sato, 1990; Mpodozis and Kay, 1990), possibly controlled by the presence of an early Paleozoic suture (Fig. 1).

Two important structures in Andean evolution were formed during the Paleozoic (Fig. 1). The La Manga lineament is interpreted to be part of a NNW-trending lithospheric anisotropy with evidence of successive reactivation of regional and discrete structural grain through the late Paleozoic to Mesozoic (Bechis et al., 2010). The Sosneado-Melipilla lineament has a WNW trend and is connected with the Melipilla anomaly proposed by Yáñez et al. (1998) in central Chile. This anomaly represents a rigid crustal block to the south of the NW-trending subvertical Melipilla sinistral shear zone of at least Early Jurassic age (Yáñez et al., 1998).

Mesozoic Extension, Volcanism, and Basin Development

In Late Permian to Early Jurassic times, the breakup of Gondwana was associated with crustal extension and thermal anomalies, leading to crustal melting and locally extensive volcanism (Llambías et al., 1993). The Late Permian to Early Triassic evolution of southwestern South America between 31°S and 36°S latitudes was characterized by the development of a great amount of bimodal volcanism under extensional conditions (Kay et al., 1989, and references therein). During the Late Triassic to Early Jurassic, extension was focused in the Neuquén Basin aperture (Vergani et al., 1995). This backarc extensional basin was characterized by the development of several isolated depocenters with distinct characteristics north and south of 35°S (Fig. 1). Early synrift deposits filling these depocenters consist of more than 2000 m of sediments north of 35°S, and more than 4000 m of volcanic and volcaniclastic rocks southward. The transition between an active rift with significant volcanism to the south and a passive rift controlled by a Paleozoic crustal anisotropy occurs at the latitudes of the Sosneado-Melipilla lineament, suggesting a strong latitudinal change in crustal strength.

Cenozoic Foreland Basins and the Andean Volcanic Arc

Neogene synorogenic strata consist of more than 2000 m of conglomerates, sandstones, and andesitic lava flows and tuffs. These rocks fill intermontane and foreland basins (Irigoyen et al., 2000; Giambiagi et al., 2003; Silvestro et al., 2005). During the early–middle Miocene, the intermontane basins formed the western edge of the foreland basins and were subsequently disconnected as deformation propagated eastward during the uplift of basement blocks, i.e., Frontal Cordillera and Bardas Blancas range, during the late Miocene.

Between 33°S and 35°S, during the early to middle Miocene, magmatic activity was located on the Chilean slope of the Principal Cordillera above a relatively thin crust (<40 km), until the Pliocene, at which time the arc migrated over 40 km east to its current location at the border between Argentina and Chile (Stern and Skewes, 1995; Kay et al., 2005). By this time, crustal thickness was in excess of 50 km (Kay and Mpodozis, 2002). South of 35°S, an important eastward arc expansion occurred between 14 and 4 Ma (Ramos and Folguera, 2011; Spagnuolo et al., 2012). Pliocene–Quaternary magmatism is represented by a volcanic arc situated in the Principal Cordillera, which has important volcanic edifices with bases located above the 3000 m elevation (Fig. 3A), and by retro-arc magmatism of the Payenia volcanic province (Bermúdez et al., 1993; Folguera et al., 2009; Ramos and Folguera, 2011). South of 35°S, Pliocene to Holocene volcanic centers are located above or immediately to the east of the Miocene magmatic arc (Kay et al., 2006).

STRUCTURAL BACKGROUND

The southern Central Andean orogen can be subdivided into a Chilean slope forearc and Argentinean slope foreland. In this paper, we focus on the thrust belts that shape the Argentinean slope of the orogen in the normal subduction segment developed south of 33°S. The Aconcagua and Malargüe fold-and-thrust belts in the Principal Cordillera (Fig. 2), where the majority of the upper-crustal shortening is accommodated (see Ramos et al., 2004), coincide with thick Mesozoic deposits of the Neuquén Basin (Fig. 1). These deposits contain mechanically weak layers that serve as décollement levels (Kozlowski et al., 1993; Manceda and Figueroa, 1995). North of 34°40′S, the NNW-trending La Manga lineament, which corresponds to a Mesozoic extensional fault, controlled the limit of deposition. East of this lineament, where the Frontal Cordillera is uplifted today, Mesozoic strata were not deposited.

The major detachment level for the Andean thrust belts in this area has been located between 10 and 12 km based on cross-section balancing and geophysical modeling (Manceda and Figueroa, 1995; Giambiagi et al., 2003, 2008, 2009; Farías et al., 2010).

We have divided the study area into three distinct structural domains (Fig. 2A), which are also coincident with the segmentation of the Southern volcanic zone followed by Kay et al. (2005) in discussing the evolution of the Neogene arc in this region. The northern domain (33°30′S–34°40′S) contains the southern sector of the Aconcagua fold-and-thrust belt, the northern sector of the Malargüe fold-and-thrust belt, and the Frontal Cordillera. This sector corresponds to a hybrid thick- and thin-skinned belt. Cross-sections A, B, and C show the interaction between newly created and preexisting basement faults with thrusts affecting the Mesozoic cover (Fig. 2B). Shortening achieved in this sector is on the order of 40%, reaching 65% locally. Deformation in the Frontal Cordillera is focused on a limited number of NNW- to NNE-trending faults present at its eastern border (Giambiagi et al., 2011).

The central domain (34°40′S–35°20′S) corresponds to the northern part of the Malargüe fold-and-thrust belt and represents a transitional zone with respect to structural and morphological characteristics (cross-sections D–F; Fig. 2B). The Malargüe fold-and-thrust belt here has been classically interpreted as a thick-skinned belt with basement thrust sheets transferring shortening to shallow detachments located in the Mesozoic strata (Kozlowski et al., 1993). The majority of the deep-seated basement structures correspond to reactivation of preexisting west-dipping early Mesozoic faults. The easternmost of these faults, the La Manga fault, a master fault developed during the extensional period of the Neuquén Basin (Bechis et al., 2010), controlled the position of the thrust front during the Andean contraction, which shows a westward location in comparison with the northern and southern sectors (Fig. 2B).

The southern sector (cross-sections G–K; Fig. 2B) is deformed by three deep-seated structures that involve the crystalline basement. They are the Malargüe and Palauco anticlines to the east and the Bardas Blancas fault system to the west (Giambiagi et al., 2009). Numerous extensional features inherited from the Triassic–Jurassic rifting episode contribute to the overall structural grain of the area (Manceda and Figueroa, 1995; Yagupsky et al., 2008; Giambiagi et al., 2009). This is especially the case in the Malargüe and Palauco areas, where preexisting normal faults are interpreted to have controlled the localization of some faults and the vergence of the compressional deformation.

STRUCTURAL AND MORPHOLOGICAL FEATURES OF THE ANDEAN THRUST BELTS

Topography

Most of the topographic relief in the Principal and Frontal Cordilleras is the result of tectonic uplift, isostatic adjustments of thickened

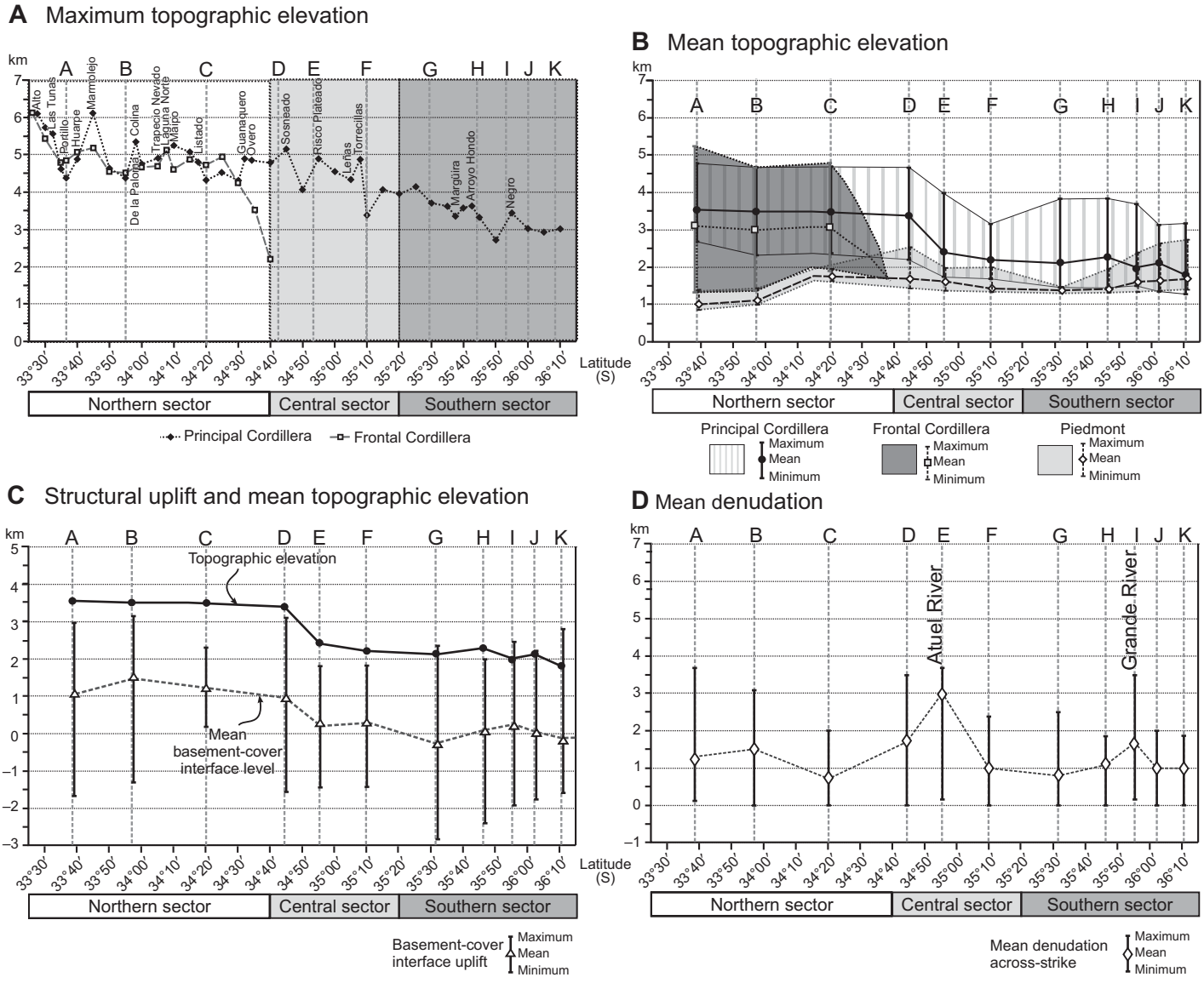

Figure 3. (A) Latitudinal distribution of maximum topographic elevation and names of the Pliocene–Holocene volcanoes. (B) Latitudinal variation in mean topographic elevation in Principal and Frontal Cordilleras and the foothills. Notice the vertical step of ~1 km around 34°50′S. (C) Comparison between the mean topographic elevation curve and the basement-cover interface curve. Notice the similarity between both curves. The diagram emphasizes the step in the mean topographic and basement-cover interface curves between 34°40′S and 35°S. (D) Latitudinal distribution in mean denudation for the Principal Cordillera. Mean denudation is in the order of 1.2 km.

crust, magmatic addition, and erosion. Summits reach elevations higher than 6 km, but mean relief is commonly 3 km (Figs. 3A–3B). The northern sector exhibits significantly greater relief and higher average elevation (Fig. 3B) than the central and southern sectors, including high rugged peaks of near 6000 m elevation corresponding to Pliocene–Quaternary volcanic edifices (Fig. 2A). Some of these volcanoes remain largely intact, indicating that rates of erosion were not high during Pliocene–Quaternary times. Miocene–Pliocene synorogenic sediments preserved between the Principal and Frontal Cordilleras (Fig. 2A) and patches of low-relief relict landscape in the Frontal Cordillera between the Río Mendoza and Río Tunuyán suggest low rates of denudation, and therefore nearly pure surface uplift, since the middle Miocene.

Along strike, there is a marked change in topographic elevation in the Principal Cordillera from an average of 3400 m in the northern sector to 2200 m in the southern sector. These elevations do not decrease steadily but instead have an important step in mean surface elevation between cross-sections D and E (34°40′S–34°53′S), in the zone where the Sosneado-Melipilla lineament crosses the study area. This topographic step correlates with the disappearance of the Frontal Cordillera south of 34°40′S (Fig. 3B).

Across strike, in the northern sector, mean elevations are similar for both Principal and Frontal Cordilleras, with an abrupt and steep transition from the Frontal Cordillera to the foothills. In the central and southern domains, where the Frontal Cordillera is absent, mean elevation decreases toward the south, from 2200 to 2000 m.

Structural Uplift and Horizontal Shortening

For each cross section, we calculated the mean structural uplift of the Principal Cordillera by averaging the height of the basement-cover interface along the cross section (Fig. 3C). The most striking feature is that the southward decrease in structural elevation mimics the southward decrease in mean topographic elevation. Taking into account the topographic step, and considering the sedimentary cover thickness, the top of the basement in the Principal Cordillera should be vertically offset by 800 m in only 20 km along strike. This is in agreement with uplift markers presented by Farías et al. (2008) in the western slope of the Principal Cordillera, indicating that the orogen was uplifted >2.5 km at 33°45′S and ~1.5 km at 34°30′S between 10.5 and 4.6 Ma.

Our reconstructions indicate that the amount of shortening systematically decreases from north to south along strike (Fig. 4A), from 55 km (39%) to 10 km (10%). The Frontal and Principal Cordilleras lineally decrease in shortening southward until they reach the central sector. In this sector, the Frontal Cordillera disappears, and shortening in the Principal Cordillera drops to 14 km. The curve for both cordilleras in Figure 4A shows that shortening decreases lineally southward, with a minimum at 35°S interrupting this general trend.

Crustal Thickness and Lithosphere Structure

Based on the 3-D Moho geometry in the model of Tassara and Echaurren (2012), we computed three parameters for each cross section. These are maximum crustal thickness, crustal root area below 40 km depth, and crustal root width (Figs. 4B, 4C, and 4D). Maximum crustal thickness and crustal root width are fairly constant along the northern sector (50 km and 325 km, respectively), and both show a notable decrease to a minimum for section D (47.5 and 275 km) into the central sector. Toward the south, the maximum crustal thickness remains roughly constant, but the crustal root width gradually increases along the central sector to values around 340 km at the southern sector. These spatial variations in maximum crustal thickness (Fig. 4B) and width of the crustal root (Fig. 4C) translate into similar variations on the crustal root cross-sectional area (Fig. 4D), which show maximum values along the northern sector (1750–2000 km^2), a regional minimum at section D (~1200 km^2), a gradual increase to a local maximum at the middle of the southern sector (sections H–I; ~1750 km^2), and then a decrease toward the southern end of the studied region (1500 km^2). Along-strike variations of the crustal structure are similar to those of topography (Fig. 3) and, in particular, to the north-south changes of geologically constrained horizontal shortening (Figs. 4A and 4E), and this suggests a common cause. There is also an important correlation among the Moho geometry, the Frontal Cordillera, and the La Manga lineament, as can be observed in Figure 1.

Figure 5 shows three lithospheric-scale E-W cross sections directly extracted from the ACHISZS electronic database (www.achiszs.udec.cl/~achiszs/accessdb.html), which allows for storage and visualization of the Tassara and Echaurren (2012) 3-D model. Subduction of the Nazca slab occurs at a constant dipping angle along the region, and the first-order structure of the upper plate, as shown by the geometry of the lithosphere-asthenosphere boundary and continental Moho, does not change significantly from north to south. However, second-order variations in the dimensions of the crustal root can be seen and are quantified in Figures 4B–4D.

Mean Denudation

Figure 3D shows the mean denudation obtained for each cross section in the Principal Cordillera, as well as maximum and minimum values. In the Frontal Cordillera, the planation surfaces in the Tunuyán and Mendoza valleys would suggest denudation to be limited to the Miocene sedimentary cover, which potentially covered the surfaces. Our data show that denudation in the Principal Cordillera is not correlated with any of the other factors analyzed. In particular, neither topographic nor structural uplift, nor horizontal shortening, presents a correlation with mean denudation, suggesting that rock uplift does not control denudation rates. In fact, 10 of the 11 cross sections show similar values of mean denudation around 1.2 km (between 0.7 and 1.6 km). Cross-sections D and E present higher values (2 and 3 km, respectively), reflecting the high denudation of the sectors in which the inversion of Late Triassic–Early Jurassic depocenters took place. This suggests that the amount of denudation is controlled primarily by the structural style of the thrust belts, but the trace of the cross sections close to the Atuel (section E) and Río Grande (section I) valleys also correlate with these high amounts of denudation.

Chronology of Deformation

Deformation in the study area started in middle to late Miocene times. Figure 4E shows a compilation of the Neogene–Quaternary geochronology data and estimated exhumation magnitudes inferred for the eastern slope of the Principal Cordillera. The chronology of shortening within the northern sector is recorded by the syntectonic sediments (Irigoyen et al., 2000; Giambiagi et al., 2003). The earliest synorogenic strata appear at ca. 18 Ma, with the source region restricted to the Principal Cordillera, but the main phase of deformation occurred between 15 and 8 Ma (Giambiagi et al., 2003). Between 9 and 6 Ma, the synsedimentary record indicates uplift of the Frontal Cordillera from 33°30′S to 34°30′S (Baldauf, 1997; Irigoyen et al., 2000; Giambiagi et al., 2003). During this time, there was a lull in deformation in the Principal Cordillera, but shortening resumed afterward, between 6 and 4 Ma, with out-of-sequence thrusting (Giambiagi and Ramos, 2002; Fock et al., 2006). Thermochronology studies (Ávila et al., 2005; Graber, 2011) show very little exhumation in this area over the Cenozoic. An apatite (U-Th)/He study in the Frontal Cordillera between 32°50′S and 33°40′S yielded pre-Miocene exhumation rates of ~12 m/m.y., with an increase to 40 m/m.y. subsequent to 25 Ma and an inferred onset of rapid river incision between 10 and 7 Ma, roughly within geologic constraints (Graber, 2011). Both of these studies point to the dearth of exhumation in the Frontal Cordillera over the Neogene.

Along the central sector, the northernmost Malargüe fold-and-thrust belt was active between 16 and 7 Ma, with a peak in deformation, concentrated along the La Manga fault, between 10.5 and 8 Ma (Giambiagi et al., 2008; Fig. 4E). Deformation practically ceased after 8 Ma. Direct and indirect evidence suggests that the easternmost part of the Malargüe fold-and-thrust belt was affected by compression during the Pleistocene. Late Pleistocene–Holocene activity on thrust faults has been extensively documented for the foothills of the Frontal Cordillera (Cortés and Sruoga, 1998; Casa et al., 2011). South of 34°40′S, deformation stopped during the Pleistocene (Giambiagi et al., 2008; Silvestro and Atencio, 2009), and there is no evidence of late Pleistocene–Holocene compressional deformation.

In the southern sector, the main episode of faulting took place between the early Miocene and late Pliocene (18–3 Ma; Giambiagi et al., 2008; Silvestro and Atencio, 2009). The deformation migrated toward the foreland over time, from 17 to 1 Ma, leaving interior faults inactive, while creating faults in the foreland basins. Undeformed Pleistocene deposits cover the structures (Giambiagi et al., 2009).

The evolution of crustal thickening can be estimated by the geochemical trend of the magmatic rocks. In the Los Andes–El Teniente area

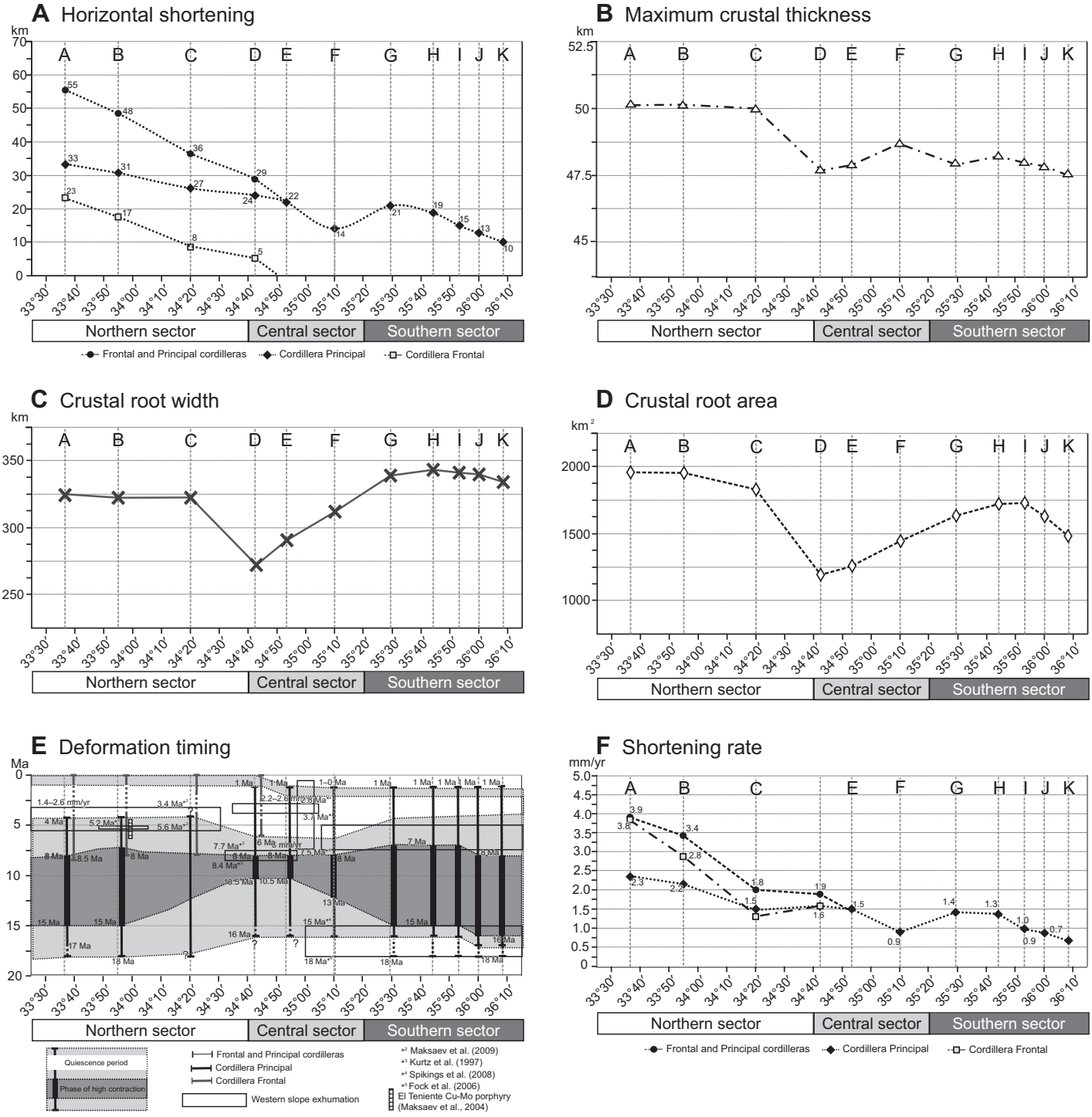

Figure 4. (A) Latitudinal distribution from north (33°30′S) to south (36°10′S) of upper-crustal horizontal shortening. White boxes represent shortening in the Frontal Cordillera, black diamonds represent shortening in the Principal Cordillera, and black spots represent shortening in both Frontal and Principal Cordilleras. The minimum value in cross-section F is inferred to be partially due to the existence of an inverted Mesozoic depocenter located toward the west, for which Andean shortening is not computed into our data. (B–D) Latitudinal distribution in maximum crustal thickness (B), crustal root width, more than 40 km thick (C), and crustal root area (D) calculated along the cross sections for 900 km from the trench toward the foreland. (E) Compilation of the Neogene–Quaternary chronology and estimated exhumation magnitudes inferred for the western slope of the Principal Cordillera. See text for references. (F). Calculated shortening rates from horizontal shortening and deformation timing. Notice that specific structures deform at a higher rate than the calculated average, for instance, the inversion of the La Manga preexisting extensional fault. *1—Giambiagi and Ramos (2002), *2—Giambiagi et al. (2008), *3—Giambiagi et al. (2009).

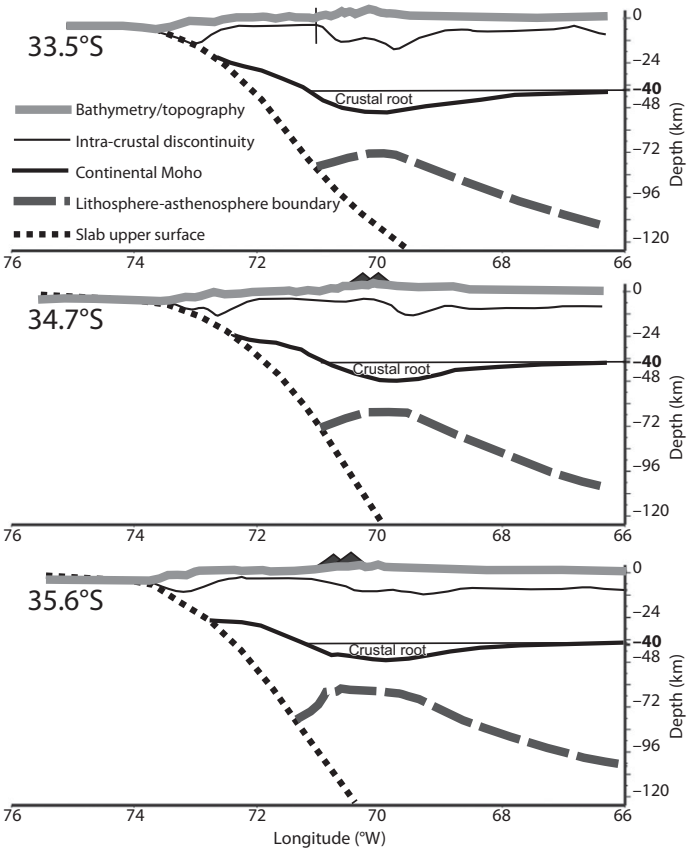

Figure 5. Three lithospheric-scale E-W cross sections (33.5°S, 34.7°S, and 35.6°S) extracted from the ACHISZS electronic database (www.achiszs.educ.cl/~achiszs/accessdb.html). Observe that the geometry of the lithosphere-asthenosphere boundary and continental Moho does not change significantly from north to south; however, second-order variations in the dimensions of the crustal root can be appreciated.

(33°S–34°30′S), in the western slope of the Andes, trace-element features of the magmatic rocks are consistent with a crustal thickness of ~30–35 km during the 37–20 Ma and 20–16 Ma periods (Nyström et al., 2003; Kay et al., 2005). This condition prevailed until 12 Ma, when the crust reached 40 km of thickness, with subsequent thickening of the crust until it reached 50 km during the 10.5–7 Ma period (Kay et al., 2005). This last period coincides with a rapid river incision in the Frontal Cordillera (Graber, 2011).

These data suggest that an important contractional event took place at ca. 10–8 Ma, coincident with the thrust front migration from the Principal Cordillera to the Frontal Cordillera north of 34°40′S, and with significant crustal thickening. From 5 to 1 Ma, there was a lull in deformation, both in the eastern and western slope of the Andes, consistent with geomorphologic evidence in the foothills of the Andes between 33°S and 34°40′S (Polanski, 1963), with geological evidence in the San Rafael block and southward, between 36°S and 38°S (Ramos and Kay, 2006; Folguera et al., 2009), and with a period of relaxation in the contractional deformation during formation of the giant El Teniente porphyry Cu-Mo deposit (34°S) from 6.5 to 4.3 Ma (Maksaev et al., 2004). During the Pleistocene, there was a reactivation of contraction deformation in the actual thrust front, all along the belts, but only the northern segment continues to deform until present day.

Deformation Rates

The southward decrease in amount of shortening is matched by a corresponding drop in the rate of shortening, which is higher in the northern sector and gradually decreases southward (Fig. 4F). This is in agreement with a greater amount (55–60 km) and higher rate of thrusting (4.7–6 mm/y) in the northern sector of the Aconcagua fold-and-thrust belt (Ramos et al., 1996) than in the southern sector (Giambiagi and Ramos, 2002). Our balanced sections and stratigraphic relationships imply average shortening rates of 3 mm/yr, 1.4 mm/yr, and 1 mm/yr for the northern, central, and southern sectors, respectively, for the Miocene–Quaternary period. There are important distinctions in the temporal variation in deformation rates among the three regions (Figs. 6D–6E). In the first stage of bulk shortening, between 18 and 10 Ma, the rate of shortening gradually diminished southward from 3 mm/yr to 0.9 mm/yr, but it has a low value zone in the central sector, with average rates of less than 1 mm/yr (Fig. 6D). This low was compensated for in the next stage, between 10 and 5 Ma, when the central sector achieved the highest rate, around 3.6 mm/yr (Fig. 6E). From 5 to 0 Ma, the rate was around 2 mm/yr and 0.5 mm/yr for the northern and southern sectors, respectively (Fig. 6F).

Our data indicate that kinematic histories are different north and south 35°S. In the north, there has been constant reactivation of thrust movements and generation of out-of-sequence thrusts, and when slip transferred to the Frontal Cordillera, shortening within the Aconcagua fold-and-thrust belt steadily slowed until it stopped around 6–4 Ma. In contrast, in the Malargüe fold-and-thrust belt, deformation migrated eastward in-sequence with minimum internal deformation of the thrust belt. Since the Pliocene, upper-plate shortening has been slow all along the belt.

COMPARISON WITH THE CHILEAN SLOPE

The onset of deformation in the Chilean slope of the Andes at these latitudes is marked by the change from low-K Abanico Formation tholeiites to calc-alkaline Farellones Formation volcanics (Kay et al., 2005, 2006). This event is diachronous, indicating that at the beginning of upper-crustal contraction, between 25 and 18 Ma, deformation was localized in the Pacific slope, with a southward migration from ca. 25 to ca. 18 Ma in the onset of thrusting (Charrier et al., 2005). In contrast, our study indicates that the onset of deformation in the Atlantic slope is constrained between 18 and 17 Ma, in agreement with studies to the south (36°S–38°S), which argue for onset of compressional deformation around 19 Ma and a coeval arc expansion eastward (Kay et al., 2006; Spagnuolo et al., 2012). By this time, there was a synchronic shift in the locus of deformation toward the east, and thrusting and uplift were concentrated in the Aconcagua and Malargüe belts. We interpret this event as the generation of an

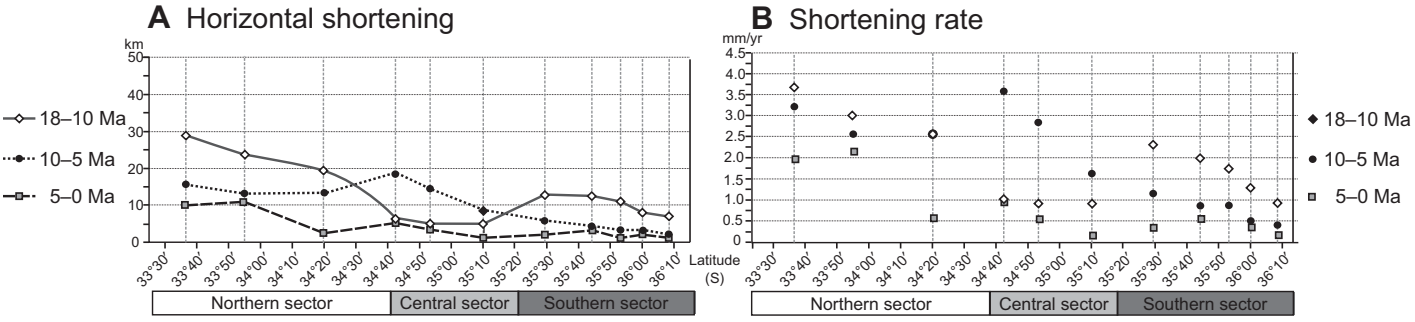

Figure 6. Diagrams showing latitudinal variations in horizontal shortening (A–C) and shortening rates (D–F), for the different periods of deformation, 18–10 Ma (A and D), 10–5 Ma (B and E), and 5–0 Ma (C and F). Notice that even though the onset of deformation does not vary from north to south, there is always a southward decrease in structural shortening and shortening rates during the three deformation periods.

important detachment connected to the Chilean ramp, as proposed by Farías et al. (2010), and located between 12 and 10 km depth beneath the Principal Cordillera.

Thermochronological studies from the Chilean slope have shown that exhumation rates increased at 33°S–34°S between 20 and 16 Ma (Kurtz et al., 1997; Fock et al., 2006), but early to middle Miocene cooling of granitoids has been interpreted as partly related to thermal relaxation of intrusions (Spikings et al., 2008; Maksaev et al., 2009). Several authors agree that the most important exhumation period took place during the late Miocene to early Pliocene, between 8 and 5 Ma, south of 35°S, and between 6 and 3 Ma northward (Spikings et al., 2008; Farías et al., 2008; Maksaev et al., 2009). This suggests that the tectonic exhumation in the Chilean slope south of 35°S (8–5 Ma) occurred immediately after the peak of upper-crust deformation in the Argentine slope (15–7 Ma) and during the last stage of eastward arc expansion (14–4 Ma); north of 35°S, tectonic exhumation in the western slope (6–3 Ma) occurred immediately after the uplift of the Frontal Cordillera (9–6 Ma) and after the crust achieved its present thickness (10.5–7 Ma).

CRUSTAL MODELS FOR THE SOUTHERN CENTRAL ANDES

Our crustal model assumes two types of crustal deformation (Fig. 7). In the northern transect (33°40′S), the crust below the Andes appears to reach its greatest thickness of 50 km at a longitude near 69°45′W (Fig. 7A). This longitude closely corresponds to the location of the highest peaks at this latitude, indicating the alignment of maximum crustal thickness, maximum topographic elevation, and upper-crustal shortening. In contrast, the southern transect (35°40′S) reaches maximum crustal thickness (47 km) at a longitude near 70°20′W, while the location of upper-crustal shortening is completely shifted toward the east near 69°56′W (Fig. 7B). The eastward migration of the volcanic arc from the Miocene to the Holocene as a consequence of crustal erosion in the forearc, as proposed by Kay et al. (2005), could explain part of this difference in orogen width, but the remainder is related to the style of the lower-crust deformation and the generation of the crustal root.

In the southern model (Fig. 7B), compensation of shortening in the upper crust, concentrated in the Argentine slope, occurs by ductile strain in the Chilean slope. Shortening of the ductile lower crust, weakened by the magmatic arc activity and undergoing distributed deformation, may have contributed to the crustal thickening of this sector. This offset shortening corresponds to the "simple shear" concept of Andean mountain building proposed by Isacks (1988). On the contrary, in the northern model, lower-crustal shortening occurs by ductile strain in the eastern slope, coincident with upper-crustal shortening.

Timing of activity for the basal detachment in both models varies. In the northern model, the detachment was active between 18 and 8 Ma, with a reactivation around 6–4 Ma. Afterward, it became inactive. In the south, the detachment was active from 18 Ma until the waning of contraction around 1 Ma.

The most obvious structural difference between both models is the absence of the Frontal Cordillera in the south. The higher structural elevation present north of 34°40′S coincides with the presence of the major basement fault that uplifts the Frontal Cordillera and the existence of a thick crust below this morphostructural unit (Fig. 7A). The southward decrease in structural uplift is explained by the absence of this deeply seated fault (Fig. 7B). The mean topographic variation can be explained if the lower crust is weaker in the northern segment and can support lower-crustal flow across strike. This explains why, in the northern sector, the location of the maximum amount of shortening in the upper crust coincides with the thickest part of the crust, while in the southern sector, the thickest crust is underneath the western Principal Cordillera.

The different deformational styles north and south of 35°S are interpreted here to be due to the pre-Andean geologic history. Previous tectonic events, such as the Permian–Triassic silicic-magmatic event and the Triassic–Jurassic development of the Neuquén Basin, modified the thickness and composition of the crust, weakening or strengthening the lithosphere. Strengthening of the lithosphere may have taken place during the Mesozoic, with substantial modification of the lower-crust composition. Thinning of the crust may have also strengthened the lithosphere in the southern sector compared to the northern sector. The Neuquén Basin south of 35°S is associated with significant crustal thinning during early Mesozoic extension (Vergani et al., 1995). In the central sector of the basin, Sigismondi (2011) proposed a crustal attenuation factor (β_c) of 1.29–1.48, with crustal thicknesses of 27 km at the center of some Triassic–Jurassic depocenters. We suggest that north of 35°S, where the Mesozoic rift was localized in a narrow NNW-trending zone, the lower crust has not been substantially modified by the rifting process. In contrast, south of 35°S, modification of the lower crust by mafic underplating (Kay et al., 1989; Llambías et al., 1993) during the opening of the Neuquén Basin, and thinning of the crust, may have strengthened it. This gain in mechanical resistance of the lower crust prevented its flow under the external compressional forces, and thus may have inhibited the Frontal Cordillera uplift. This effect may have been strengthened by the eastward expansion of the magmatic arc south of 35°S, promoting the development of an upper-crustal detachment.

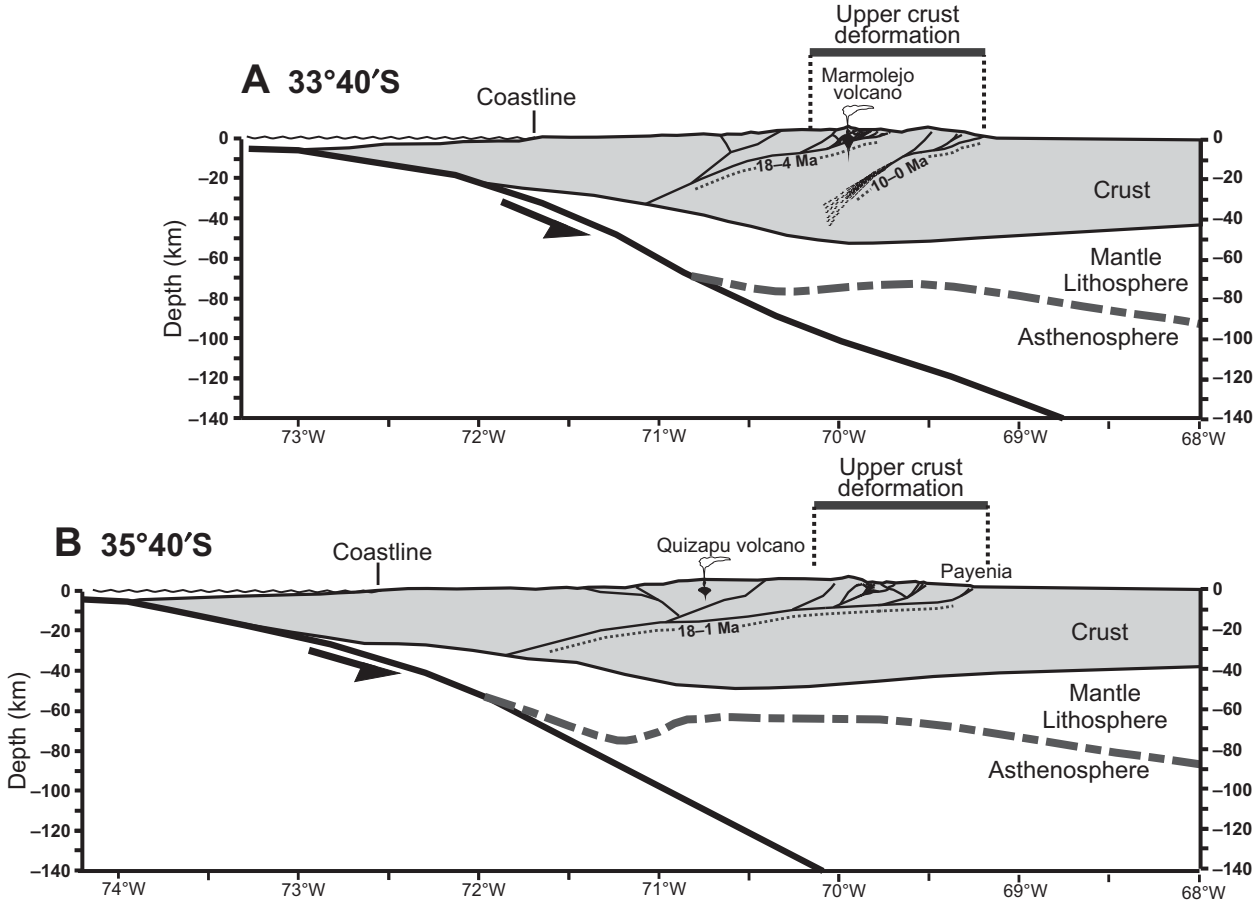

Figure 7. Conceptual models for the 33°40′S (A) and 35°40′S (B) crustal deformation styles. (A) The northern model shows a coupling between upper-crustal brittle deformation and lower-crustal ductile deformation, and an alignment between the localization of brittle deformation and the maximum crustal thickness. (B) In the southern model, the upper-crustal shortening, located in the Atlantic slope of the Andes, is uncoupled from the ductile lower-crustal deformation zone, present in the Pacific slope of the Andes.

DISCUSSION

Causes of Along-Strike Variation in Mean Topographic Uplift

Our data show a remarkable step in topographic elevation in the central domain (34°40′S–35°20′S) coinciding with the southward disappearance of the Frontal Cordillera and notable changes in crustal root width and crustal area. The structural elevation of the basement-cover interface, which is an isostatic response to the crustal deformation and thickening, crustal density modifications, and the lithospheric thermal state, mimics the present topographic uplift, while mean denudation is low and does not vary broadly along strike. On the other hand, crustal shortening and thickness steadily diminish southward, with local second-order variations in the lineal decrease. Therefore, our data indicate that other factors apart from upper-crustal shortening are associated with the creation of topography in the Andean orogen.

The response of topographic elevation to tectonics, climate and erosion has been emphasized in the last three decades (Strecker et al., 2007, and references therein). To see if erosional processes play an important role in the kinematics of deformation of the thrust belts and mean topographic uplift, here we look at the mean denudation variations along the strike of the Principal Cordillera and compare them with shortening amounts, structural uplift, and mean topography. The analysis indicates a dearth of denudation in the Principal Cordillera that, combined with studies from the Frontal Cordillera, suggests nearly pure surface uplift in the Argentine slope, while available data in the Chilean slope suggest more rock uplift. Our analysis demonstrates that denudation and topographic uplift variations are not directly correlated, nor is the horizontal shortening directly related to mean topography. In this way, we do not obtain a direct feedback between erosional processes and tectonics for the Atlantic slope of the southern Central Andes

The topographic step at 35°S is inferred here to be related to the deformation style and the coupling between upper- and lower-crustal deformation. This degree of coupling is governed by the crustal strength, which in turn is ruled by its pre-Andean history. Our results indicate that pre-Andean history, especially initial crustal thickness and lower-crustal composition, exerts a fundamental control on the distribution of topography.

Causes of Along-Strike Variation in Shortening

The southern Central Andes show remarkable latitudinal variations in horizontal shortening. Although there are several proposed

explanations for this variation, the mechanism of these southward drops remains debatable. In our study area, we can rule out a control by diachronous onset of deformation (Spikings et al., 2008), since the age of deformation is constrained between 18 and 17 Ma. A control by variations of coupling at the interplate slip zone, given by the age of the subducting plate through its effect on the thermally controlled viscosity of the slip zone, has also been proposed (Yáñez and Cembrano, 2004), and may be applicable on a regional scale. However, for a smaller scale, such as the 300-km-long study segment, the age of the Nazca plate at the trench is fairly constant around 35 Ma, suggesting that the eventual role of subducting plate thermal structure on interplate coupling can be ruled out.

On the other hand, lithospheric strength variations exerted by the inherited crustal-scale geological structure do play an important role in upper-crustal dynamics. The question arises, however, whether changes in the lithospheric strength could have an impact over the amount of shortening a crust can achieve. Oncken et al. (2006) suggested that the shortening rate of the upper plate reflects changes in the integral strength of the overriding lithosphere; weakening of the upper plate should enhance shortening. Tassara and Yáñez (2003) proposed that the southward decrease of contraction in the Central Andes is due to a more mafic bulk composition of the crust and therefore a stronger lithosphere. In this way, the Mesozoic Neuquén Basin development could have an important impact on the lithospheric strength during the Andean deformation. However, regional studies for the entire Central Andes point out this pattern of southward decrease in shortening (e.g., Kley and Monaldi, 1998), indicating that the development of a Mesozoic basin is not responsible for this feature at a regional scale, and therefore it may play a role in our study area, but it is not the only factor controlling shortening amounts at the regional scale.

Further north in the Central Andes, it has been suggested that thick sedimentary basins promote the formation of thin-skinned thrust belts and thus facilitate shortening (Allmendinger and Gubbels, 1996; Kley et al., 1999). Both the Aconcagua and Malargüe fold-and-thrust belts coincide with thick Mesozoic deposits containing multiple stratigraphic horizons that serve as detachments. All along and across the study area, except in its northeastern sector, Mesozoic sediments are up to 4 km thick; therefore, our data do not show a correlation between presence of thick Mesozoic–Cenozoic strata and the amount of shortening, meaning that the amount of contraction a crust can achieve is not related to the presence of thick strata.

We propose that the overall crustal shortening of the southern Central Andes may be largely controlled by orogen-scale dynamics of the lithosphere and subduction system. We observe a lineal decrease in crustal shortening southward, indicating that interplate dynamics may control the overall pattern of tectonic shortening. Local variations, however, shed some light on the influence of controlling factors over local variations in the amount of shortening. The curve for both cordilleras in Figure 5A shows that shortening decreases lineally southward, with a minimum of shortening at 35°S interrupting this general trend. This minimum is interpreted here as reflecting local upper-crustal strength variations due to Neuquén Basin development.

CONCLUSIONS

In this paper, we analyzed latitudinal variations in structural and morphological features of the Argentine slope of the southern Central Andes, between 33°S and 36°S. These features correspond to upper-crustal shortening, style of deformation, structural uplift of the basement, crustal root geometry, and maximum and mean topographic elevations. We also compared temporal variation in the structural shortening and rate of deformation by integrating all previous geochronological and thermochronological data. The amount of crustal shortening gradually diminishes southward, and this decrease has been persistent over the different stages of deformation in the Argentine slope since the early-middle Miocene (18–17 Ma) to the Holocene. Our results suggest that this large-scale decrease in shortening can be mostly explained by the dynamics of the interplate contact between the Nazca and South American plates, but we outline that the mechanical properties of the upper plate have a first-order control over crustal geometry and mean topographic uplift, and a second-order control over local variations in amount of shortening. This particularly includes those mechanical heterogeneities that are due to the Paleozoic tectonic events and the development of the Mesozoic Neuquén rift basin. In particular, the inherited distribution of the Triassic–Jurassic Neuquén Basin and its opening mechanism represent major controlling factors on the Andean deformational style, and this in turn controls the topographic uplift. Contrasting crustal inheritance such as crustal thickness and lower-crust composition may be responsible for the difference in the degree of coupling between upper- and lower-crustal deformation. The perfect match between crustal root thickness and width with the location of maximum average topographic elevation allows us to propose that the degree of coupling between the brittle upper-crustal and the ductile lower-crustal deformation is a first-order control over the mean topographic uplift.

To account for the morphological and structural step at around 35°S, we propose two models of crustal deformation. In the northern model, bulk upper-crustal shortening in the Aconcagua fold-and-thrust belt and the Frontal Cordillera is compensated by the ductile generation of a crustal root below these mountain ranges. In this way, upper-crustal shortening is not detached from lower-crustal shortening, as indicated by the position of the crustal root. In the southern segment, bulk shortening in the Malargüe fold-and-thrust belt is compensated by distributed, ductile shortening beneath the Chilean slope of the orogen. These models explain some important morphological features present in the southern Central Andes. In particular, they can explain the lack of a broad correlation between surface topography and amount of shortening in both Principal and Frontal Cordilleras north of 34°40′S.

ACKNOWLEDGMENTS

This research was supported by grants from the CONICET (PIP 638 and PIP 5843) and the Agencia de Promoción Científica y Tecnológica (PICT 07-10942) to Giambiagi, and National Science Foundation (OISE-0601957) to Hoke. Giambiagi, Mescua, Bechis, Tassara, and Hoke are part of International Geoscience Programme (IGCP) 586-Y "Geodynamic Processes in the Andes," funded by IGCP and United Nations Educational, Scientific, and Cultural Organization (UNESCO). Victor Ramos and an anonymous reviewer are sincerely thanked for their critical and helpful comments and suggestions.

REFERENCES CITED

Allmendinger, R.W., and Gubbels, T., 1996, Pure and simple shear plateau uplift, Altiplano-Puna, Argentina and Bolivia: Tectonophysics, v. 259, p. 1–13, doi:10.1016/0040-1951(96)00024-8.

Ávila, J.N., Chemale, F., Mallmann, G., Borba, A.W., and Luft, F.F., 2005, Thermal evolution of inverted basins: Constraints from apatite fission track thermochronology in the Cuyo Basin, Argentine Precordillera: Radiation Measurements, v. 39, p. 603–611, doi:10.1016/j.radmeas.2004.08.009.

Azcuy, C.L., and Caminos, R., 1987, Diastrofismo, *in* Archangelsky, S., ed., El Sistema Carbonífero en la República Argentina: Córdoba, Argentina, Academia Nacional de Ciencias (Argentina), p. 239–252.

Baldauf, P., 1997, Timing of the Uplift of the Cordillera Principal, Mendoza Province, Argentina [M.Sc. thesis]: Washington, D.C., George Washington University, 356 p.

Bechis, F., Giambiagi, L., García, V., Lanés, S., Cristallini, E., and Tunik, M., 2010, Kinematic analysis of a transtensional fault system: The Atuel depocentre of the Neuquén Basin, Central Andes, Argentina: Journal of Structural Geology, v. 32, p. 886–899, doi:10.1016/j.jsg.2010.03.009.

Bermúdez, A., Delpino, D., Frey, F., and Saal, A., 1993, Basaltos de retroarco extraandinos, *in* Ramos, V.A., ed., Relatorio Geología y Recursos Naturales de la Provincia de Mendoza, 12th Congreso Geológico Argentino: Buenos Aires, Servicio Geológico Minero Argentino (SEGEMAR), Abstracts, v. 1, p. 161–172.

Casa, A., Cortés, J.M., and Rapalini, A., 2011, Fallamiento activo y modificación del drenaje en el piedemonte del cordón del Carrizalito, Mendoza, *in* Proceedings of the 18th Congreso Geológico Argentino, Neuquén, Abstracts: Buenos Aires, Servicio Geológico Minero Argentino (SEGEMAR), v. 1, p. 712–713.

Charrier, R., Bustamante, M., Comte, D., Elgueta, S., Flynn, J.J., Iturra, N., Muñoz, N., Pardo, M., Thiele, R., and Wyss, A.R., 2005, The Abanico extensional basin: Regional extension, chronology of tectonic inversion, and relation to shallow seismic activity and Andean uplift: Neues Jahrbuch für Geologie und Paläontologie, v. 236, p. 43–77.

Cortés, J.M., and Sruoga, P., 1998, Zonas de fractura cuaternarias y volcanismo asociado en el piedemonte de la Cordillera Frontal (34°30′S), Argentina, *in* Proceedings of the 10th Congreso Latinoamericano de Geología, and 6th Congreso Nacional de Geología Económica, Buenos Aires: Buenos Aires, Servicio Geológico Minero Argentino (SEGEMAR), v. 2, p. 116–121.

Farías, M., Charrier, R., Carretier, S., Martinod, J., Fock, A., Campbell, D., Cáceres, J., and Comte, D., 2008, Late Miocene high and rapid surface uplift and its erosional response in the Andes of central Chile (33°–35°S): Tectonics, v. 27, TC1005, doi:10.1029/2006TC002046.

Farías, M., Comte, D., Charrier, R., Martinod, J., David, C., Tassara, A., Tapia, F., and Fock, A., 2010, Crustal-scale structural architecture in Central Chile based on seismicity and surface geology: Implications for Andean mountain building: Tectonics, v. 29, TC3006, doi: 10.1029/2009TC002480.

Fock, A., Charrier, R., Maksaev, V., Farías, M., and Alvarez, P., 2006, Evolución cenozoica de los Andes de Chile Central (33°–34°S), *in* Proceedings of the 9th Congreso Geológico Chileno, Antofagasta: Santiago, Servicio Nacional de Geología y Minería (SERNAGEMIN), v. 2, p. 205–208.

Folguera, A., Naranjo, J.A., Orihashi, Y., Sumino, H., Nagao, K., Polanco, E., and Ramos, V., 2009, Retroarc volcanism in the northern San Rafael block (34°–35°30′S), southern Central Andes: Occurrence, age, and tectonic setting: Journal of Volcanology and Geothermal Research, v. 186, p. 169–185, doi:10.1016/j.jvolgeores.2009.06.012.

Giambiagi, L., and Ramos, V.A., 2002, Structural evolution of the Andes between 33°30′ and 33°45′S, above the transition zone between the flat and normal subduction segment, Argentina and Chile: Journal of South American Earth Sciences, v. 15, no. 1, p. 101–116, doi:10.1016/S0895-9811(02)00008-1.

Giambiagi, L., Ramos, V.A., Godoy, E., Alvarez, P.P., and Orts, S., 2003, Cenozoic deformation and tectonic style of the Andes, between 33° and 34° south latitude: Tectonics, v. 22, no. 4, 1041, doi:10.1029/2001TC001354.

Giambiagi, L., Bechis, F., García, V., and Clark, A., 2008, Temporal and spatial relationship between thick- and thin-skinned deformation in the Malargüe fold and thrust belt, southern Central Andes: Tectonophysics, v. 459, p. 123–139, doi:10.1016/j.tecto.2007.11.069.

Giambiagi, L., Ghiglione, M., Cristallini, E., and Bottesi, G., 2009, Kinematic models of basement/cover interactions: Insights from the Malargüe fold and thrust belt, Mendoza, Argentina: Journal of Structural Geology, v. 31, p. 1443–1457, doi:10.1016/j.jsg.2009.10.006.

Giambiagi, L., Mescua, J., Bechis, F., Martínez, A., and Folguera, A., 2011, Pre-Andean deformation of the Precordillera southern sector, southern Central Andes: Geosphere, v. 7, no. 1, p. 219–239, doi:10.1130/GES00572.1.

Graber, N.R., 2011, Uplift of the Argentine Frontal Cordillera through (U-Th)/He thermochronology and geomorphic analysis [M.S. thesis]: Syracuse, New York, Syracuse University, 60 p.

Irigoyen, M.V., Buchan, K.L., and Brown, R.L., 2000, Magnetostratigraphy of Neogene Andean foreland-basin strata, lat 33°S, Mendoza Province, Argentina: Geological Society of America Bulletin, v. 112, p. 803–816, doi:10.1130/0016-7606(2000)112<803:MONAFS>2.0.CO;2.

Isacks, B., 1988, Uplift of the Central Andean plateau and bending of the Bolivian orocline: Journal of Geophysical Research, v. 93, p. 3211–3231, doi:10.1029/JB093iB04p03211.

Jordan, T.E., Isacks, B.L., Allmendinger, R.W., Brewer, J.A., Ramos, V.A., and Ando, C.J., 1983, Andean tectonics related to geometry of subducted Nazca plate: Geological Society of America Bulletin, v. 94, p. 341–361, doi:10.1130/0016-7606(1983)94<341:ATRTGO>2.0.CO;2.

Kay, S.M., and Mpodozis, C., 2002, Magmatism as a probe to the Neogene shallowing of the Nazca plate beneath the modern Chilean flat-slab: Journal of South American Earth Sciences, v. 15, p. 39–57, doi:10.1016/S0895-9811(02)00005-6.

Kay, S.M., Ramos, V.A., Mpodozis, C., and Sruoga, P., 1989, Late Paleozoic to Jurassic silicic magmatism at the Gondwana margin: Analogy to the Middle Proterozoic in North America?: Geology, v. 17, p. 324–328, doi:10.1130/0091-7613(1989)017<0324:LPTJSM>2.3.CO;2.

Kay, S.M., Godoy, E., and Kurtz, A., 2005, Episodic arc migration, crustal thickening, subduction erosion, and magmatism in the south-central Andes: Geological Society of America Bulletin, v. 117, no. 1–2, p. 67–88, doi:10.1130/B25431.1.

Kay, S.M., Burns, M., Copeland, P., and Mancilla, O., 2006, Upper Cretaceous to Holocene magmatism and evidence for transient Miocene shallowing of the Andean subduction zone under the northern Neuquén Basin, *in* Kay, S.M., and Ramos, V.A., eds., Evolution of an Andean Margin: A Tectonic and Magmatic View from the Andes to the Neuquén Basin (35°–39°S lat): Geological Society of America Special Paper 407, p. 19–60.

Kley, J., and Monaldi, C.R., 1998, Tectonic shortening and crustal thickness in the Central Andes: How good is the correlation?: Geology, v. 26, p. 723–726, doi:10.1130/0091-7613(1998)026<0723:TSACTI>2.3.CO;2.

Kley, J., Monaldi, C.R., and Salfity, J.A., 1999, Along-strike segmentation of the Andean foreland: Causes and consequences: Tectonophysics, v. 301, p. 75–94, doi:10.1016/S0040-1951(98)90223-2.

Kozlowski, E., Manceda, R., and Ramos, V.A., 1993, Estructura, *in* Ramos, V.A., ed., Relatorio Geología y Recursos Naturales de Mendoza: 12th Congreso Geológico Argentino, and 2nd Congreso de Exploración de Hidrocarburos, Buenos Aires: Buenos Aires, Servicio Geológico Minero Argentino (SEGEMAR), v. 1, p. 235–256.

Kurtz, A., Kay, S., Charrier, R., and Farrar, E., 1997, Geochronology of Miocene plutons and exhumation history of the El Teniente region, Central Chile (34°–35°S): Revista Geológica de Chile, v. 24, p. 73–90.

Lamb, S., and Davis, P., 2003, Cenozoic climate change as a possible cause for the rise of the Andes: Nature, v. 425, p. 792–797, doi:10.1038/nature02049.

Llambías, E.J., and Sato, A.M., 1990, El batolito de Colangüil (28°–31°S), Cordillera Frontal de Argentina, estructura y marco tectónico: Revista Geológica de Chile, v. 17, p. 89–108.

Llambías, E.J., Kleinman, L.E., and Salvarradi, J.A., 1993, El magmatismo Gondwánico, *in* Ramos, V.A., ed., Relatorio Geología y Recursos Naturales de Mendoza: 12th Congreso Geológico Argentino, and 2nd Congreso de Exploración de Hidrocarburos, Mendoza: Buenos Aires, Servicio Geológico Minero Argentino (SEGEMAR), v. 1, p. 53–64.

Maksaev, V., Munizaga, V.F., McWilliams, M., Fanning, M., Mathur, R., Ruiz, J., and Zentilli, M., 2004, New chronology for El Teniente, Chilean Andes, from U-Pb, $^{40}Ar/^{39}Ar$, Re-Os and fission-track dating: Implications for the evolution of a supergiant porphyry Cu-Mo deposit, *in* Sillitoe, R.H., Perelló, J., and Vidal, C.E., eds., Andean Metallogeny: New Discoveries, Concepts and Updates: Society of Economic Geologists Special Publication 11, p. 15–54.

Maksaev, V., Munizaga, F., Zentilli, M., and Charrier, R., 2009, Fission track thermochronology of Neogene plutons in the Principal Andean Cordillera of central Chile (33–35°S): Implications for tectonic evolution and porphyry Cu-Mo mineralization: Andean Geology, v. 36, p. 153–171, doi:10.4067/S0718-71062009000200001.

Manceda, R., and Figueroa, D., 1995, Inversion of the Mesozoic Neuquén rift in the Malargüe fold-thrust belt, Mendoza, Argentina, *in* Tankard, A.J., Suárez, R., and Welsink, H.J., eds., Petroleum Basins of South America: American Association of Petroleum Geologists Memoir 62, p. 369–382.

Mescua, J.F., 2010, Evolución Estructural y Tectónica del Area Comprendida entre Las Choicas y Santa Elena, Cordillera Principal de Mendoza [Ph.D. thesis]: Buenos Aires, Universidad de Buenos Aires, Facultad de Ciencias Exactas y Naturales, 241 p.

Mescua, J.F., and Ramos, V.A., 2009, Estratigrafía y estructura de las nacientes del Río Borbollón, alto Río Diamante, Provincia de Mendoza: Revista de la Asociación Geológica Argentina, v. 65, no. 1, p. 111–122.

Mpodozis, C., and Kay, S.M., 1990, Provincias magmáticas ácidas y evolución tectónica de Gondwana: Andes Chilenos (28°–31°S): Revista Geológica de Chile, v. 17, p. 153–180.

Mpodozis, C., and Ramos, V.A., 1989, The Andes of Chile and Argentina, *in* Ericksen, G.E., Cañas, M.T., and Reinemund, J.A., eds., Geology of the Andes and its Relation to Hydrocarbon and Mineral Resources: Circum-Pacific Council for Energy and Mineral Resources, Earth Science Series 11, p. 59–90.

Nyström, J., Parada, M.A., and Vergara, M., 2003, Sr-Nd isotope compositions of Cretaceous to Miocene volcanic rocks in central Chile: A trend towards a MORB signature and a reversal with time, *in* 2nd International Symposium on Andean Geodynamics, Oxford: Paris, Institut de Recherche pour le Development (IRD), v. 1, p. 21–23.

Oncken, O., Hindle, D., Kley, J., Elger, K., Victor, P., and Schemmann, K., 2006, Deformation of the central Andean upper plate system—Facts, fiction, and constraints for plateau models, *in* Oncken, O., Chong, G., Franz, G., Giese, P., Götze, H.-J., Ramos, V.A., Strecker, M.R., and Wigger, P., eds., The Andes—Active Subduction Orogeny: Berlin, Springer-Verlag, Frontiers in Earth Science Series, Volume 1, p. 3–27.

Polanski, J., 1963, Estratigrafía, neotectónica y geomorfología del Pleistoceno pedemontano, entre los Ríos Diamante y Mendoza: Revista de la Asociación Geológica Argentina, v. 17, no. 3–4, p. 127–349.

Ramos, V.A., 1988, The tectonics of the Central Andes (30°–33°S latitude), *in* Clark, S., Burchfiel, D., and Suppe, D., eds., Processes in Continental Lithospheric Deformation: Geological Society of America Special Paper 218, p. 31–54.

Ramos, V.A., 2010, The tectonic regime along the Andes: Present-day and Mesozoic regimes: Geological Journal, v. 45, p. 2–25, doi:10.1002/gj.1193.

Ramos, V.A., and Folguera, A., 2011, Payenia volcanic province in the Southern Andes: An appraisal of an exceptional Quaternary tectonic setting: Journal of Volcanology and Geothermal Research, v. 201, p. 53–64, doi:10.1016/j.jvolgeores.2010.09.008.

Ramos, V.A., and Kay, S.M., 2006, Overview of the tectonic evolution of the southern Central Andes of Mendoza and Neuquén (35°–39°S latitude), *in* Kay, S.M., and Ramos, V.A., eds., Evolution of an Andean Margin: A Tectonic and Magmatic View from the Andes to the Neuquén Basin (35°–39°S Lat): Geological Society of America Special Paper 407, p. 1–18.

Ramos, V.A., Cegarra, M.I., and Cristallini, E., 1996, Cenozoic tectonics of the High Andes of west-central Argentina (30–36°S latitude): Tectonophysics, v. 259, p. 185–200, doi:10.1016/0040-1951(95)00064-X.

Ramos, V.A., Zapata, T., Cristallini, E., and Introcaso, A., 2004, The Andean thrust system: Latitudinal variations in structural styles and orogenic shortening, *in* McClay, K.R., ed., Thrust Tectonics and Hydrocarbon Systems: American Association of Petroleum Geologists Memoir 82, p. 30–50.

Sheffels, B., 1990, Lower bound on the amount of crustal shortening in the Central Bolivian Andes: Geology, v. 18, p. 812–815, doi:10.1130/0091-7613(1990)018<0812:LBOTAO>2.3.CO;2.

Sigismondi, M.E., 2011, El estiramiento cortical de la Cuenca Neuquina: Modelo de cizalla simple, *in* 18th Congreso Geológico Argentino, Neuquén, Abstracts: Servicio Geológico Minero Argentino (SEGEMAR), Buenos Aires, v. 1, p. 858–859.

Silvestro, J., and Atencio, M., 2009, La cuenca Cenozoica del Río Grande y Palauco: Edad, evolución y control estructural, faja plegada de Malargüe (36°S): Revista

de la Asociación Geológica Argentina, v. 65, no. 1, p. 154–169.

Silvestro, J., Kraemer, P., Achilli, F., and Brinkworth, W., 2005, Evolución de las cuencas sinorogénicas de la Cordillera Principal entre 35°–36°S, Malargüe: Revista de la Asociación Geológica Argentina, v. 60, no. 4, p. 627–643.

Spagnuolo, M.G., Litvak, V.D., Folguera, A., Bottesi, G., and Ramos, V., 2012, Neogene magmatic expansion and mountain building processes in the southern Central Andes, 36–37°S, Argentina: Journal of Geodynamics, v. 53, p. 81–94, doi:10.1016/j.jog.2011.07.004.

Spikings, R., Dungan, M., Foeken, J., Carter, A., Page, L., and Stuart, F., 2008, Tectonic response of the central Chilean margin (35–38°S) to the collision and subduction of heterogeneous oceanic crust: A thermochronological study: Journal of the Geological Society of London, v. 165, p. 941–953, doi:10.1144/0016-76492007-115.

Stern, C.R., and Skewes, M.A., 1995, Miocene to Present magmatic evolution at the northern end of the Andean Southern volcanic zone: Central Chile: Revista Geológica de Chile, v. 22, p. 261–271.

Strecker, M.R., Alonso, R.N., Bookhagen, B., Carrapa, B., Hilley, G.E., Sobel, E.R., and Trauth, M.H., 2007, Tectonics and climate of the southern Central Andes: Annual Review of Earth and Planetary Sciences, v. 35, p. 747–787, doi:10.1146/annurev.earth.35.031306.140158.

Tassara, A., and Yáñez, G., 2003, Relación entre el espesor elástico de la litósfera y la segmentación tectónica del margen andino (15–47°S): Revista Geológica de Chile, v. 30, p. 159–186.

Tassara, A. and Echaurren, A., 2012, Anatomy of the Andean subduction zone: three-dimensional density model upgraded and compared against global-scale models: Geophysical Journal International, v. 189, p. 161–168.

Tassara, A., Götze, H.-J., Schmidt, S., and Hackney, R., 2006, Three-dimensional density model of the Nazca plate and the Andean continental margin: Journal of Geophysical Research, v. 111, B09404, doi:10.1029/2005JB003976.

Turienzo, M., 2010, Structural style of the Malargüe fold-and-thrust belt at the Diamante River area (34°30′–34°50′S) and its linkage with the Cordillera Frontal Andes of central Argentina: Journal of South American Earth Sciences, v. 29, p. 537–556, doi:10.1016/j.jsames.2009.12.002.

Vergani, G.D., Tankard, J., Belotti, J., and Welsink, J., 1995, Tectonic evolution and paleogeography of the Neuquén Basin, Argentina, *in* Tankard, A.J., Suárez, R., and Welsink, H.J., eds., Petroleum Basins of South America: American Association of Petroleum Geologists Memoir 62, p. 383–402.

Yagupsky, D., Cristallini, E., Fantín, J., Zamora Valcarce, G., Bottesi, G., and Varadé, R., 2008, Oblique half-graben inversion of the Mesozoic Neuquén rift in the Malargüe fold and thrust belt, Mendoza, Argentina: New insights from analogue models: Journal of Structural Geology, v. 30, p. 839–853, doi:10.1016/j.jsg.2008.03.007.

Yáñez, G.A., and Cembrano, J., 2004, Role of viscous plate coupling in the Late Tertiary Andean tectonics: Journal of Geophysical Research, v. 109, B02407, doi:10.1029/2003JB002494.

Yáñez, G.A., Gana, P., and Fernández, R., 1998, Origen y significado geológico de la anomalía Melipilla: Chile Central: Revista Geológica de Chile, v. 25, no. 2, p. 175–198.

Science Editor: Christian Koeberl
Associate Editor: J. Duncan Keppie

Manuscript Received 19 September 2011
Revised Manuscript Received 16 December 2011
Manuscript Accepted 22 December 2011

Printed in the USA